Electron-Ion Recombination in Dense Plasmas*

EINAR HINNOV AND JOSEPH G. HIRSCHBERG
Plasma Physics Laboratory, Princeton University, Princeton, New Jersey
(Received August 29, 1961)

The rate of recombination and the characteristics of the afterglow line emission have been measured in magnetically confined plasmas of helium and hydrogen, with electron densities of the order of 10^{13} cm^{-3} and degree of ionization initially of the order of 50%. Electron densities and temperatures are deduced from absolute intensity measurements of spectrum line intensities originating from highly excited states, in good agreement with those obtained from microwave phase shift and plasma conductivity measurements. The results are explained in terms of an electron-electron-ion three-body recombination process. The recombination coefficient for this process is calculated as a function of electron temperature and density.

INTRODUCTION

RECOMBINATION rates in dense plasmas have been studied in the past in the afterglows of arc discharges,[1] electrodeless discharges[2] and hollow cathode discharges.[3] The observed rates always exceed those expected from two-body radiative recombination, often by several orders of magnitude. Some of the results have been explained, with varying degrees of success, in terms of ionic molecule formation and subsequent dissociative recombination.[4]

The present experiments were carried out in the magnetically confined plasma in the quiescent afterglow of the *B*-1 stellarator discharge. The experimental conditions differ from those of previous measurements by considerably lower neutral densities, and practical absence of diffusion of charged particles to the walls. Under these conditions the formation of ionic molecules should be greatly inhibited, and any residual ionic molecules, as in hydrogen discharge, may be expected to disappear early in the afterglow through the fast mechanism of dissociative recombination.

Preliminary reports on the results have been published previously.[5,6] This paper will summarize the results to date, and present our views of the mechanism responsible for the observed rates of recombination.

EXPERIMENTAL RESULTS

The experimental work has been performed on the *B*-1 stellarator,[7] the details of which are not especially relevant for the purposes of this paper. The experimental system could be represented by a long cylinder of 4.8 cm diameter, with an axial magnetic field of 23 kgauss. The system is initially filled with the gas under consideration, at a pressure of the order of 1 μ Hg, and ionized by means of an alternating electric field to a degree of ionization of 40–80%. The observations consisted of the measurement of spectrum line intensities and electron densities, at right angles to the axis of the tube, immediately after terminating the ionizing field.

The time-resolved intensities of the emitted spectrum lines were measured with a 0.5-cm Jaco Ebert type monochromator, equipped with a 1P21 RCA photomultiplier. The photomultiplier output was displayed on an oscillograph screen and photographed. The entire optical and detection system has been calibrated against a standard tungsten ribbon lamp for absolute intensity measurements, with an estimated accuracy of about 20% in the wavelength range of 3500–6000 A. This accuracy is comparable to the day-to-day reproducibility of the stellarator output, and to the reading accuracy of the intensity of the weaker lines.

The electron densities were determined from measurements of phase shifts of a 4.3-mm microwave beam transmitted across the tube. The estimated accuracy of the electron density measurements is about 30% in the range 5×10^{13}–10^{12} cm^{-3}.

Typical behavior of the light intensity is shown in Fig. 1, for several lines of helium. The top half of the figure shows the lines corresponding to $2\,^3P$–$3\,^3D$ and $2\,^3P$–$5\,^3D$ transitions. Time direction is from right to left, scale 2 divisions per millisecond. The first peak corresponds to electronic excitation during the ionizing phase of about 1-msec length, which is followed by a dark gap, and the afterglow emission caused by the recombination. The gap is roughly inversely proportional to the starting pressure, and represents the initial rapid cooling of the electrons. The decay of the afterglow is exponential with time, with a time constant given roughly, for neutral helium, $t=(1\text{ msec})\times P^{-\frac{1}{2}}$, where P is the initial helium pressure in μ Hg. (The λ4026 light does not look exponential on this picture, but the difference is only initial. Following the intensity down shows the exponential behavior, under some

* Work performed under the auspices of the U. S. Atomic Energy Commission.
[1] C. Kenty, Phys. Rev. **32**, 624 (1928); F. L. Mohler, Bur. Standards J. Research **19**, 447, 559 (1937).
[2] M. A. Biondi and S. C. Brown, Phys. Rev. **75**, 1700 (1949).
[3] C. R. Burnett, Bull. Am. Phys. Soc. **6**, 188 (1960).
[4] D. R. Bates, Phys. Rev. **77**, 718 (1950); Phys. Rev. **78**, 492 (1950); M. A. Biondi, Phys. Rev. **83**, 1078 (1951); M. Bayet, Compt. rend. **232**, 612 (1951); M. A. Biondi and T. D. Holstein, Phys. Rev. **82**, 962 (1951); R. A. Johnson, B. T. McClure and R. B. Holt, Phys. Rev. **82**, 103 (1951); W. A. Rogers, Westinghouse Research Laboratory Report 6-94439-7-R6, 1958 (unpublished); D. E. Kerr (private communication).
[5] A. F. Kuckes, R. W. Motley, E. Hinnov, and J. G. Hirschberg, Phys. Rev. Letters **6**, 337 (1961).
[6] E. Hinnov and J. G. Hirschberg, *Proceedings of the Fifth International Conference on Ionic Phenomena, Munich, 1961* (North-Holland Publishing Company, Amsterdam, 1961).
[7] T. Coor *et al.*, Phys. Fluids **1**, 411 (1958).

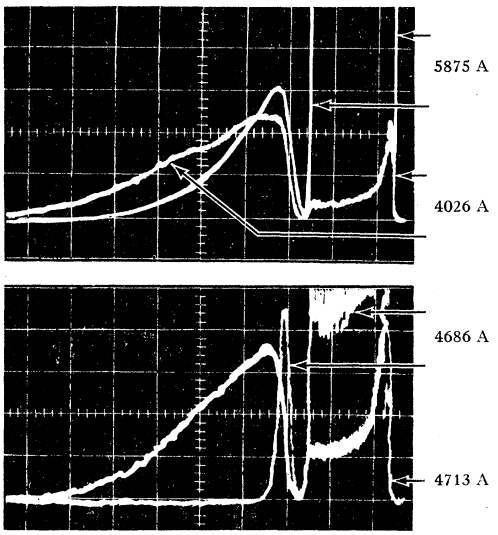

FIG. 1. Typical results on line intensity measurements in helium afterglow.

conditions over several decades). The electron density time dependence in this interval is also exponential, with the same time constant as the light intensity.

Except for the above-mentioned pressure dependence, the time behavior of the light intensity and electron density is independent of all other conditions of the plasma, such as the strength and duration of the ionizing phase, the strength of the confining magnetic field, or moderate amounts of argon, hydrogen, carbon, or carbon monoxide impurities.

The lower part of Fig. 1 shows the relationship between the afterglow of the ionized and neutral helium light. In the ionized helium the afterglow peaks somewhat before the neutral helium afterglow and decays exponentially, with a time constant more than ten times shorter than that of the neutral helium. The afterglow time behavior of impurity ions in helium discharges is very similar to that of the helium ion, while the hydrogen impurity (the only neutral impurity observed in the helium discharge) behaves like the neutral helium. All time constants are observed to change with the initial pressure, as described above, and are apparently unaffected by other conditions of the plasma.

Qualitatively very similar results have been obtained with pure hydrogen discharges, except that stronger exciting fields, and somewhat higher pressures were necessary to produce afterglows of sufficient intensity. Temperature measurements show that under these conditions the electron temperature is higher during the discharge, and falls more rapidly in the afterglow, than in the helium under comparable conditions. In the light corresponding to lower excited levels of hydrogen, another peak appears in what corresponds to the dark gap, the maximum occurring less than 100 μsec after shunting the excited fields, followed by rapid decay of the intensity. This light has been tentatively ascribed to dissociative recombination of residual molecular ions.

Some afterglow measurements have been also performed with argon. Because of the complicated spectrum of argon and the general lack of knowledge of the transition probabilities, no extensive analysis of the recombination process in argon has been feasible. However, the temperature, electron density and afterglow light intensity time behavior has been found to be very similar to that of helium under comparable conditions.

Another feature shown in Fig. 1 is the relative intensity during the discharge and the afterglow. In the λ5875 light, the intensity during the discharge, produced by electronic excitation, is off the picture entirely, i.e., considerably higher than the afterglow peak, while in the λ4026 light it is somewhat lower than the afterglow peak. This behavior is quite general, although less pronounced at higher pressures. At still higher initial states of excitation, the afterglow intensity becomes much larger relative to the intensity during the discharge. This fact provides a practically conclusive indication of the origin of the afterglow in a process of recombination and, furthermore, in a process that is not dissociative recombination of an intermediate molecular ion.[8] Other evidence, supporting the same conclusion, includes the following observations. The ratio of singlet to triplet intensities in the helium afterglow is closely 1:3. The fact that hydrogen impurity in the helium afterglow exhibits the same behavior as neutral helium shows that the same process must be operative in both. Since the afterglow in pure hydrogen discharge behaves in a noticeably different manner, the important characteristics of the afterglow plasma, e.g., electron temperature and density, must be determined by the dominant component of the discharge. There is a lack of evidence of any molecular compounds in the helium discharge, except trace amounts of CO. An addition of about 1% CO impurity to the helium discharge did not produce any noticeable difference in the time behavior of the neutral helium afterglow. Finally, from absolute intensity measurements, it has been determined that a photon is emitted for substantially every disappearing electron, showing that diffusion to the walls, as well as any recombination process involving nonradiative transitions into $n=1$ and $n=2$ states cannot play an important part in the afterglow.

The $2\,^3P$–$n\,^3D$ series in neutral helium afterglow was sufficiently intense to allow reasonably accurate measurements to $n=13$ at the higher pressures, and to about $n=10$ at the lower pressures. Figure 2 shows a representative graph of the population densities of the $n\,^3D$ states, calculated from the measured absolute intensities,

[8] In dissociative recombination, it should be expected that one particular state, or at most a small number of states should be preferentially populated, depending on the state or states of the molecule responsible for the process. In order to explain the observed populations, such as those shown in Fig. 2 and Table I, in terms of dissociative processes, a considerable number of *ad hoc* assumptions would be required.

versus E_n, the energy of the n-th state, measured from the ionization level. The three curves represent the N_n at the peak of the afterglow, and 0.5 and 1.0 millisecond later. The most important feature of these curves is the fact that for $n \gtrsim 6$ the points lie on a straight line with a slope that changes in time. This implies that those states are in transient thermal equilibrium at a temperature given by the Boltzmann equation

$$kT = \Delta E_n / \Delta \ln N_n. \quad (1)$$

Qualitatively similar results are obtained at lower helium pressures, except that the temperatures are somewhat lower, and fall less rapidly in time.

The temperatures thus measured agree with the free electron temperatures, obtained from the plasma conductivity measurements, within better than the experimental errors.[9]

Since the high-energy states are in equilibrium with the plasma electrons, the measured populations may be used to calculate the free electron densities from the Saha equation, assuming that the positive ions are all He^+, thus

$$N_e = [N_n (g_i g_e / g_n)(2\pi mkT/h^2)^{\frac{3}{2}} \exp(-E_n/kT)]^{\frac{1}{2}}, \quad (2)$$

where g_i, g_e, and g_n are the statistical weights of the ion ground state, the free electron, and the ^3D bound state, and other symbols have their conventional meaning.

Again, the electron densities thus calculated are in excellent agreement with the densities determined from microwave phase-shift measurements. It is therefore concluded that the high-energy states, $n > 5$, are populated by the three-body electron-ion recombination,

$$He^+ + e + e \rightarrow He^* + e, \quad (3)$$

and its inverse process, the ionization of the excited states through electron impact.

Application of the three-body recombination theory, proposed by several authors,[10] whereby the electrons in excited states thus populated recombine through radiative cascading, immediately showed that the theory was inadequate to explain the observed facts. Aside from numerical discrepancies, it was especially difficult to account for the relatively large populations of the lower excited levels, $n = 4$ and 3. Subsequent calculations showed that radiative cascading from higher levels constitute an almost negligible contribution to the recombination coefficient, except at relatively low temperatures and electron densities. The major contribution arises from transitions between bound states through superelastic and inelastic collisions with electrons. The following section presents an investigation of the predominant features of the recombination coefficient.

[9] R. W. Motley and A. F. Kuckes, *Proceedings of the Fifth International Conference on Ionic Phenomena, Munich, 1961* (North-Holland Publishing Company, Amsterdam, 1961).

[10] N. D'Angelo, Phys. Rev. **121**, 505 (1961); R. G. Giovanelli, Australian J. Sci. Research **A1** 274, 289 (1948).

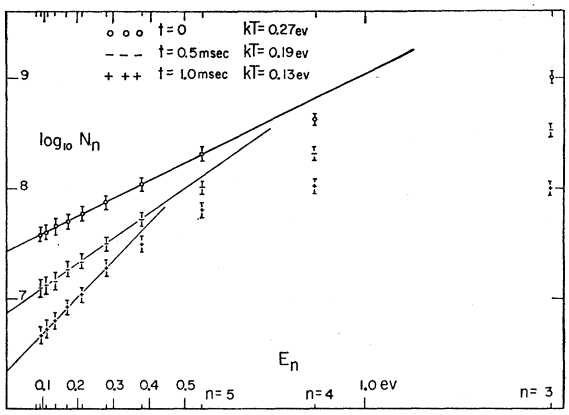

FIG. 2. Population density vs energy of the $n\,^3D$ states from measured intensities of the $2\,^3P$–$n\,^3D$ series in helium afterglow.

RECOMBINATION PROCESS

After an electron has been transferred to an energy state E_n through a three-body collision (Eq. 3), it may either be reionized through electron impact, or transferred to another bound state, either through inelastic collisions with electrons, or by radiative transitions. It is clear that at any given n there is a definite probability, generally a function of electron temperature and density, that the electron will eventually recombine (i.e., to the ground state). If the rate of ionization from the nth level is larger than the net downward transition rate, the level will be in Saha equilibrium with the free electrons. Under given conditions, there are generally only a few levels that are of critical importance to the rate or recombination; these are in the neighborhood where equilibrium is being just established. At much higher levels, the probability of eventual recombination becomes negligible, while at much lower levels all the electrons will recombine. In principle, the rate of recombination may be calculated by solving a number of simultaneous equations, expressing the populations at the levels, N_n, in terms of each other, and the various collisional and radiative transition probabilities. This is a rather tedious calculation, and in view of the uncertainties in the collisional transition probabilities, perhaps not worth the effort at present. Instead, we have attempted to obtain a reasonable approximation to the recombination coefficient, by applying a number of simplifying assumptions.

In the subsequent calculations, the various substates of a given n-level are assumed to be kept at thermal equilibrium with respect to each other by electron collision, i.e., their relative populations are taken to be given by the Boltzmann distribution function. Whenever the substates have appreciably different energies, a weighted average is used for the energy of the level, E_n, and the appropriate transition probabilities. Experimental justification for this assumption will be discussed later.

We first assume that the collisional transition

probability from the continuum to level n, ${}^{\infty}C_n$, is a function increasing with n, and that the probability $P_1{}^n$, that an electron in state n will eventually recombine, decreases with increasing n so that[11]

$$\sum_{n=1}^{\infty} {}^{\infty}C_n P_1{}^n$$

is finite. We may then define a "critical" level n^* by

$$\sum_{1}^{n^*} {}^{\infty}C_n = \sum_{n=1}^{\infty} {}^{\infty}C_n P_1{}^n. \tag{4}$$

Physically, n^* is a level such that the number of electrons transferred above it from the continuum which eventually recombine is equal to the number transferred below it, which subsequently will be reionized. Presumably, n^* is a function of electron temperature and density.

If the electron temperature is small, the levels important to the recombination coefficient occur at large n, where $E_n \gg E_{n,n-1}$, the energy separation of adjacent levels. Therefore we expect the collisional transition probabilities between adjacent bound levels to be much larger than the probability of reionization, and the probabilities of radiative transitions much smaller than either. If the collisional transition probability from n to $n-1$ is ${}^nC_{n-1}$, the reverse probability will be ${}^nC_{n-1}(g_n/g_{n-1})\exp(-E_{n,n-1}/kT)$. As n increases, the upward transition probability will increase with respect to the downward transition probability. Since both terms are much larger than ${}_nC^{\infty}$, the ionization probability from level n, we might expect that the "critical" level n^* should be given by the condition

$$(g_n/g_{n-1})\exp(-E_{n,n-1}/kT)=1. \tag{5}$$

Solving for $n=n^*$ from this equation, using the condition $n^* \gg 1$, yields

$$n^* \approx (13.6/kT)^{\frac{1}{2}} \quad \text{or} \quad E_n{}^* \approx kT, \tag{6}$$

where kT is given in electron volts. The condition $n^* \gg 1$ implies $kT \lesssim 0.25$ ev. As long as the electron densities are sufficiently high, so that radiative transitions are negligible in the neighborhood of n^*, the latter is independent of N_e.

An electron with energy E passing a bound electron with an impact parameter d, transfers an energy E_s according to the classical Thomson formula,[12]

$$d_s{}^2 = e^4 E^{-1}(E_s{}^{-1} - E^{-1}). \tag{7}$$

We take the ionization cross-section from level n to be given by $\pi d_n{}^2$ as given by Eq. (7) when E_s is replaced by E_n. Multiplying by the electron energy distribution function and integrating, the rate of ionization from n is given by

$$N_n N_e \pi e^4 (8/\pi m)^{\frac{1}{2}} kT^{-\frac{3}{2}} \int_{x_n}^{\infty} (x_n{}^{-1} - x^{-1}) \exp(-x) dx, \tag{8}$$

where $x = E/kT$. With $E_n \approx kT$, the value of the integral is approximately $(2/5)x_n \exp(-x_n)$, and the ionization rate is

$${}_nC^{\infty}N_n = (4/5)\pi e^4 (2/\pi m kT)^{\frac{1}{2}} E_n{}^{-1} \exp(-E_n/kT) N_n N_e. \tag{9}$$

The rate of the inverse process is obtained by substituting for N_n the equilibrium value from the Saha equation because the two rates must be equal at equilibrium. Summing over n from $n=1$ to $n=n^*$ gives then the rate of recombination. With numerical values

$$-\partial N_e/\partial t = \alpha N_e{}^2 = 4.2\times 10^{-29} kT^{-2} N_e{}^3 \sum_{n=1}^{n^*} n^4, \tag{10}$$

where kT is given in electron volts. Since $n^* \gg 1$ the sum may be replaced with the integral over n. Substituting n^* from Eq. (6), finally yields

$$\alpha \approx 5.6\times 10^{-27} kT^{-9/2} N_e \text{ cm}^3 \text{ sec}^{-1}. \tag{11}$$

At low electron densities the assumption that radiative transition probabilities are negligible in the neighborhood of n^* no longer holds, and we might expect the recombination coefficient to be somewhat larger than Eq. (11) predicts. However, it appears that radiative recombination will become predominant before this happens. The total recombination coefficient at low temperatures will therefore be taken as

$$\alpha = \alpha_C + \alpha_R. \tag{12}$$

With α_C given by Eq. (11), and α_R by[13]

$$\alpha_R \approx 2.7\times 10^{-13} kT^{-3/4} \text{ cm}^3 \text{ sec}^{-1}. \tag{13}$$

Because of the various assumptions and approximations involved in the derivation of α_C, the numerical constant may be regarded accurate only to a factor 2 or so. However, the temperature and density variation of α_C should be essentially correct.

At temperatures higher than about 0.25 ev most of the assumptions involved in derivation of n^* break down, and Eq. (11) predicts generally too high values for the recombination coefficient. The main reason for this is that ${}_nC^{\infty}$ becomes comparable, or even larger than the transition probabilities between bound states in the region of interest.

Instead of trying to modify the expression for n^*, we shall take a different approach in the temperature range $0.25 < kT < 1$ ev. In a previous paper[6] we gave an approximate formula for the rate of recombination in

[11] Each term in this sum represents the probability of transition, in units of sec^{-1}, of an electron from the continuum to the ground state of the recombining ion through a particular path, at given electron and ion densities, which are implicit in ${}^{\infty}C_n$. When multiplied by the electron density, the sum gives the total rate of recombination in cm^{-3} sec^{-1}.

[12] J. J. Thomson, Phil. Mag. 47, 337 (1924).

[13] C. W. Allen, *Astrophysical Quantities* (The Athlone Press, London, 1955).

terms of the collisional and radiative transition probabilities between bound states. This formula predicts that for $N_e \gtrsim 5\times10^{13}$ cm^3, the $n=4$ state is approximately in Saha equilibrium with the free electrons. This conclusion is also supported by experiment: the $t=0$ graph in Fig. 2 corresponds to $N\approx5\times10^{13}$ cm^{-3}. Under these conditions, the rate of recombination is given approximately by

$$-\partial N_e/\partial t \approx N_4^{eq}\,{}^4C_3/[1+{}_3C^4/({}^3C_2+A_2{}^3)], \quad (14)$$

where $A_2{}^3$ is the radiative transition probability from $n=3$ to $n=2$, and N_4^{eq} is the equilibrium population of $n=4$, calculated from the Saha equation.

The collisional transition probabilities were calculated with substantially the same assumptions as were used in deriving Eqs. (8) and (9), yielding[6] ${}^4C_3=1.1\times10^{-6}N_e$, ${}_3C^4={}^4C_3(g_4/g_3)\exp(-E_{4,3}/kT)$, and ${}^3C_2=9\times10^{-8}N_e$.

The radiative transitions from $n=3$ to $n=1$ in Eq. (14) are ignored for the following reasons. If the neutral density is high, the $A_1{}^3$ coefficient is effectively reduced by trapped resonance radiation. If the neutral density is sufficiently small for the plasma to be transparent, the population of the ^1P levels (in helium) will be reduced, because the electron density is then also likely to be low enough to prevent rapid transitions to the ^1P from the adjacent substates. Thus in most practical cases the effect of $A_1{}^3$ is not important to the rate of recombination. Radiative transitions from higher levels to $n=1$, 2, are also of very minor importance under the conditions in consideration.

Examining Eq. (14) it is seen that at very large N_e, ${}^3C_2 \gg A_2{}^3$, the denominator is independent of N_e, and α is proportional to N_e. ($N_4^{eq}/N_e{}^2$ is independent of N_e.) As N_e decreases, so that ${}^3C_2$ becomes comparable to $A_2{}^3$, the denominator decreases with N_e, although less rapidly than the numerator. Still further decrease of N_e will make the second term in the denominator small, and α again proportional to N_e. Thus in a curve logα vs logN_e there is a "kink" with a minimum slope given by $2/[1+(1+{}_4C^3/{}^3C_2)^{\frac{1}{2}}]$ which occurs at an electron density such that $A_2{}^3={}^3C_2(1+{}_3C^4/{}^3C_2)^{\frac{1}{2}}$. It will be noted that the minimum slope increases, and therefore the amplitude of the kink decreases, with decreasing temperature.

Figure 3 shows the calculated recombination coefficient as a function of electron densities. The graphs for $kT=0.2$ and smaller have been calculated from Eq. (12). For $kT=0.3$ ev and larger, α is calculated from Eq. (14) to $N_e=2\times10^{13}$ cm^{-3}. At lower electron densities, the graph is simply extrapolated, assuming α proportional to N_e, and added to the radiative coefficient, Eq. (13). Thus it is possible that the graphs shown for $kT=0.3$ and 0.5 ev are slightly too low between $N_e=10^{12}$ and 10^{13} cm^{-3}. Similarly, the $kT=0.2$ ev curve is perhaps slightly too high at $N_e>10^{13}$ cm^{-3}. However, the discrepancies should not exceed a factor 2.

The "kink" is evident on the two curves at $kT=0.3$ and 0.5 ev. At 1.0 ev it disappeared on addition of the radiative component. At $kT=0.2$ ev it was too small to be included in the present approximation.

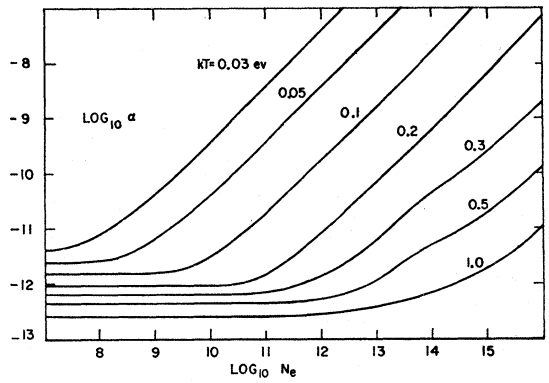

FIG. 3. Calculated recombination coefficient at different electron temperatures.

If these graphs were to be extended to higher electron densities, those for $kT \ll E_{3,2}$ would continue indefinitely. At $kT=0.3$ ev and higher, there would be another, more pronounced kink, depending on the relative magnitudes of ${}_2C^3$, ${}^2C_1$, and $A_1{}^2$, the latter to be modified by trapped resonance radiation. Thereafter all states $n\geq2$ would be in equilibrium, and the recombination rate would be

$$-\partial N_e/\partial t = N_2^{eq}\,{}^2C_1, \quad (15)$$

which again corresponds to α proportional to N_e. It should be noted that the extreme right-hand edge of Fig. 3, $N_e\approx10^{16}$ cm^{-3} corresponds to the situation where $n=3$ is in equilibrium, and α could be given alternatively by Eq. (14) with all indices reduced by one.

Equations (14) (for $n=3$) and (15) should also be applicable at higher temperatures. If the temperature becomes comparable to $E_{2,1}$, the recombination coefficient will be further reduced by a factor $1-(g_2/g_1)\exp(-E_{2,1}/kt)$.

Although the presented calculations were performed for helium or hydrogen, they may be expected to apply reasonably well to other singly ionized atoms, and even molecules, especially at lower temperatures where the important processes occur at highly excited hydrogen-like states. In molecules, of course, there exists the possibility of dissociative recombination, which probably will completely mask the electron-ion recombination under most circumstances.

No attempt has yet been made to calculate the recombination coefficient for multiply ionized atoms. It can only be stated that the coefficient will be much larger, probably by a factor about Z^4, at given electron densities and temperatures.

In the preceding calculations, it was assumed that the electron and ion densities were equal. If several species of ions are present, the partial recombination coefficients are obtained simply by substituting N_eN_i for $N_e{}^2$ in the Saha equation, and Eq. (10).

TABLE I. Comparison of measured and calculated population densities in various helium afterglows.

Transition	λ (A)	Population densities in cm^{-3} Calc.	Meas.	Calc.	Meas.	Calc.	Meas.
$2\,^3P$–$3\,^3S$	7065	6.2×10^8	1×10^9	8.0×10^7	1.5×10^8	5.1×10^6	...
$2\,^1P$–$3\,^1D$	6678	2.8×10^8	3.2×10^8	3.3×10^7	2.6×10^7	1.5×10^6	$\approx2\times10^6$
$2\,^3P$–$3\,^3D$	5875	8.5×10^8	1.0×10^9	1.0×10^8	1.4×10^8	4.3×10^6	$\approx5\times10^6$
$2\,^1P$–$4\,^1S$	5047	4.1×10^7	5.0×10^7	8.3×10^6	9.6×10^6	9.5×10^5	8.7×10^5
$2\,^1S$–$3\,^1P$	5015	1.7×10^8	1.8×10^8	2.0×10^7	9.2×10^6	8.8×10^5	2.2×10^5
$2\,^1P$–$4\,^1D$	4921	1.6×10^8	1.7×10^8	3.1×10^7	2.6×10^7	3.3×10^6	2.1×10^6
$2\,^3P$–$4\,^3S$	4713	1.6×10^8	1.5×10^8	3.3×10^7	2.7×10^7	4.0×10^6	2.9×10^6
$2\,^3P$–$4\,^3D$	4471	4.7×10^8	4.3×10^8	9.3×10^7	2.9×10^7	9.8×10^6	8.9×10^6
$2\,^1P$–$5\,^1S$	4438	1.5×10^7	2.2×10^7	3.2×10^6	4.8×10^6	5.6×10^5	7.2×10^5
$2\,^1P$–$5\,^1D$	4388	6.5×10^7	8.9×10^7	1.4×10^7	1.7×10^7	2.4×10^6	2.5×10^6
$2\,^1P$–$6\,^1D$	4144	3.7×10^7	4.9×10^7	8.3×10^6	1.0×10^7	1.4×10^6	1.7×10^6
$2\,^3P$–$5\,^3S$	4121	5.0×10^7	7.6×10^7	1.1×10^7	1.7×10^7	2.0×10^6	2.6×10^6
$2\,^3P$–$5\,^3D$	4026	2.0×10^8	2.1×10^8	4.3×10^7	4.6×10^7	7.2×10^6	7.2×10^6
$2\,^1S$–$4\,^1P$	3965	9.4×10^7	7.8×10^7	1.8×10^7	1.2×10^7	2.0×10^6	8.1×10^5
$2\,^3S$–$3\,^3P$	3888	6.3×10^8	4.3×10^8	7.6×10^7	6.3×10^7	3.5×10^6	3.4×10^6
$2\,^1S$–$5\,^1P$	3614	3.9×10^7	3.4×10^7	8.6×10^6	7.0×10^6	1.4×10^6	9.8×10^5
$2\,^3S$–$4\,^3P$	3188	3.1×10^8	2.0×10^8	6.3×10^7	4.6×10^7	6.7×10^6	4.6×10^6
Initial pressure		3.8 μ Hg		1.2 μ Hg		0.4 μ Hg	
N_e (cm^{-3})		5.5×10^{13}		2.3×10^{13}		5×10^{12}	
kT (ev)		0.27		0.25		0.20	

Finally, the results presented here appear to be in substantial agreement with a recent calculation by Bates and Kingston.[14] Minor discrepancies are probably attributable to the assumed collision cross-sections. In comparison with the calculation of D'Angelo,[10] our results predict a considerably stronger dependence of the recombination coefficient on both the electron density and the temperature.

Another recent calculation by McWhirter,[15] although performed for considerably higher temperatures, and including multiply charged ions, appears to predict slightly higher values for the recombination coefficient, but is qualitatively in good agreement with our results. The discrepancy is again apparently in the inelastic collision cross sections used in the calculations.

COMPARISON WITH EXPERIMENT

The expected population densities of various excited states in helium, at different temperatures and electron densities, have been calculated by the following procedure. Starting from a level (usually $n=6$) that is known from experiment (e.g., Fig. 2) to be in equilibrium with the free electrons, the total populations of the three lower levels are evaluated essentially by solving simultaneously equations of the type

$$N^6({}^6C_5+A_5{}^6)+N_4({}_4C^5)=N_5({}^5C_4+{}_5C^6+A_4{}^5).$$

Details of the calculations, and the collisional transition probabilities are published elsewhere.[6] The populations of the substates are then calculated from the level population according to the Boltzmann distribution function.

The populations thus obtained are compared with those from measured absolute line intensities in Table I. The calculated values are practically within the error limit of the measurements. Although the agreement may be to some extent fortuitous, it appears to be sufficient confirmation of the validity of the underlying assumptions.

The populations of the ^3S states are affected considerably by the assumption of thermal equilibrium among the substates. Unfortunately the measurements are not sufficiently good to establish the point definitely, but states such as ^3S and ^3D appear to be in equilibrium with respect to each other. With some refinement of the measuring apparatus, it may be possible to use line pairs λ4713–4471 and λ4121–4026 for measurement of electron temperature at high electron densities.

With respect to ^1P states, at higher neutral densities where radiation trapping is important, equilibrium appears to be established. At lower neutral densities the ^1P states are depopulated by rapid radiative transitions, the effect being more noticeable at lower n values, as expected. As it was mentioned before, these discrepancies are not expected to have noticeable influence on the rate of recombination, which proceeds predominantly through states of higher orbital quantum numbers.

Table II presents a comparison of measured recombination coefficients, with those extrapolated from Fig. 3. The first three column identify the conditions at the time of the measurements. The electron densities and temperatures on the authors' measurements are determined from the $\log N_n$ vs E_n curves (Fig. 2), in the measurements by Motley and Kuckes,[9] from microwave phase shifts and plasma conductivity measurements. In general, the agreement is considered to be very good, except for the first measurement at low pressure by Motley and Kuckes. However, this particular measure-

[14] D. R. Bates and A. E. Kingston, Nature **189**, 652 (1961).
[15] R. W. P. McWhirter, Nature **190**, 902 (1961).

ment was taken very early in the afterglow, when the plasma may not yet have been sufficiently quiescent.

There is a considerable number of other experiments, but all substantially over the same range of electron densities and temperatures, which therefore merely confirm the data presented in Table II.

In order to have some indication of the validity of the Eq. (11) over a wider range, we have calculated from the equation the temperatures needed to produce the observed N_e and $-\partial N_e/\partial t$ in some of the graphs by Motley and Kuckes.[9] A typical result is shown in Fig. 4. The solid curve is the measured electron density; the dashed curve, the calculated temperature. Unfortunately there are no measured temperatures at very low densities, nor are we able to calculate the expected temperature independently with sufficient accuracy. At least, we may say the temperature behavior appears reasonable.

To summarize, the present experimental observations are in good agreement with theoretical predictions. The observed time behavior of electron densities and afterglow intensities is a consequence of the time behavior

TABLE II. Comparison of measured and calculated recombination coefficients, in units of $cm^3\ sec^{-1}$.

Element	N_e (cm^{-3})	kT (ev)	P (μHg)	α_{meas}	α_{calc}
He	5.6×10^{13}	0.27	3.8	4×10^{-11}	6×10^{-11}
	1.8×10^{13}	0.19	···	1.3×10^{-10}	1.5×10^{-10}
	6.2×10^{12}	0.13	···	3.6×10^{-10}	3.6×10^{-10}
	2.3×10^{13}	0.25	1.2	5.3×10^{-11}	5×10^{-11}
	1.2×10^{13}	0.19	···	1.0×10^{-10}	1.1×10^{-10}
	6.6×10^{12}	0.15	···	1.8×10^{-10}	1.9×10^{-10}
	3.6×10^{12}	0.12	···	3.3×10^{-10}	2.8×10^{-10}
	3.6×10^{13}	0.23	10	7.3×10^{-11}	9×10^{-11}
H	4.7×10^{12}	0.11	2.0	5.5×10^{-10}	5.6×10^{-10}
	7.4×10^{12}	0.13	4.0	5.8×10^{-10}	4.5×10^{-10}
He[a]	6.2×10^{12}	0.21	0.5	1.3×10^{-10}	4×10^{-11}
	3.1×10^{12}	0.12	···	2.7×10^{-10}	2.7×10^{-10}
	1.5×10^{12}	0.09	···	5.6×10^{-10}	5.1×10^{-10}
	6.5×10^{11}	0.075	···	7×10^{-10}	5.5×10^{-10}
	1.8×10^{13}	0.21	4.0	1.3×10^{-10}	1.0×10^{-10}
	1.2×10^{13}	0.17	···	1.9×10^{-10}	2×10^{-10}
	6.1×10^{12}	0.13	···	3.7×10^{-10}	3.1×10^{-10}
	3.1×10^{12}	0.1	···	7.3×10^{-10}	5.5×10^{-10}
	1.6×10^{12}	0.066	···	1.4×10^{-9}	2×10^{-9}

[a] Measurements by Motley and Kuckes, reference 9.

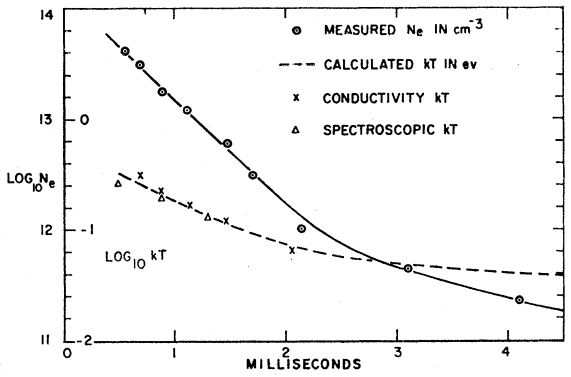

FIG. 4. Comparison of observed electron temperatures with those calculated from measured N_e and $-\partial N_e/\partial t$ according to Eq. (11).

of the electron temperature. The latter is presumably determined by energy exchange between electrons and ions, ions and neutrals, neutrals and the walls of the vessel, and further complicated by an energy feedback through superelastic collisions during the recombination process itself. There have been attempts to calculate the time dependence of the electron temperature,[5,9] but uncertainties in the various cross sections, especially of the metastable destruction and metastable reflectivity of the walls, have only permitted the conclusion that the observed behavior is not impossible.

ACKNOWLEDGMENTS

We wish to express our appreciation to Dr. R. W. Motley, Dr. A. F. Kuckes, and Dr. W. Bernstein whose investigations on the plasma losses on the B-1 stellarator led to the work described here. Dr. Motley has also been of considerable assistance in the measurement and interpretation of the microwave data. Dr. A. Z. Kranz has been helpful in running the stellarator. We are also indebted for several informative discussions and criticisms to Dr. L. Spitzer, Jr., Dr. M. B. Gottlieb, and especially Dr. N. D'Angelo who first drew our attention to recombination through electron-electron collisions.